

# Innovative and sustainable solar cells based on abundant elements on the Earth crust

STEFANO PASINI, GIANLUCA FOTI, ANTONELLA PARISINI, DONATO SPOLTORE,  
ROBERTO FORNARI and ALESSIO BOSIO

*Department of Mathematical, Physical and Computer Science, University of Parma  
Parma, Italy*

STEFANO MARCHIONNA

*Ricerca Sistema Energetico - RSE Spa, Milan, Italy*

**Summary.** — Antimony selenide is a very promising material for photovoltaic applications, with the potential to become a competitive alternative to more traditional silicon, CdTe and CIGS-based technologies. A notable feature of  $\text{Sb}_2\text{Se}_3$  is its strong anisotropy, and this property is reflected in the performance parameters of the solar cell. In this study a novel method is explored to control the grain orientation and its effects on the photovoltaic parameters of the solar cells. Furthermore, an innovative approach to create a low-resistivity, Ohmic back-contact is presented, which is crucial for enhancing the efficiency and performance of  $\text{Sb}_2\text{Se}_3$ -based solar cells.

## 1. – Introduction

Nowadays, renewable technologies, especially photovoltaics, have gained a strong boost both in terms of social interest and scientific research. Indeed, this technology can play a fundamental role in terms of energy production to satisfy the increasing energy demand and, at the same time, it allows to maintain a high level of quality of life.

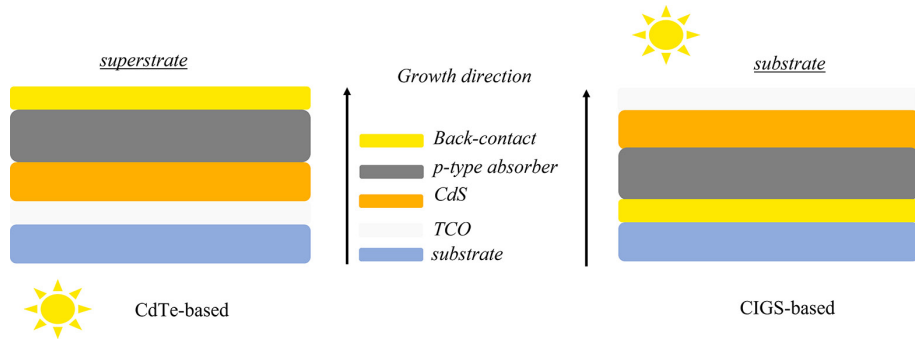


Fig. 1. – Typical superstrate and substrate configurations of CdTe- and CIGS-based solar cells.

Inorganic-solar-cells technology includes three main categories: bulk, epitaxy, and thin film. The bulk category refers to the silicon single junction based on mono- (m-Si) or polycrystalline (p-Si) materials, achieving a power conversion efficiency (PCE) of 26.8% and 24.4%, respectively [1]. To obtain high-efficiency m-Si-based solar cells it is necessary to grow silicon with a high degree of purity (9N) and typically the Czochralski method is used [2,3]. From an industrial point of view, this method is energy- and time-consuming. From the point of view of the material properties, the main disadvantages of Si are: its indirect band gap, which implies a low absorption coefficient ( $\alpha \sim 10^2\text{--}10^4 \text{ cm}^{-1}$ ) [4] and high surface reflectivity ( $R \sim 30\text{--}35\%$ ) [5], which strongly reduces solar-cell performance if surface texturing, and antireflecting coatings are not used [5-7]. Epitaxial technology is based on gallium arsenide (GaAs) and related compounds, such as InGaP and InGaS. The main growth techniques used to obtain epitaxial layers are Chemical Vapor Deposition (CVD), Molecular Beam Epitaxy (MBE) and Atomic Layer Deposition (ALD). These techniques make it possible to obtain films with optimal crystalline quality, starting from small-size germanium substrates. Given the inherent size and costs, these solar cells can be conveniently used only in concentration photovoltaic power systems. The PCE record is 47.1% under the  $143\times$  concentration system and 37.9% at one Sun [8]. On the other hand, the deposition techniques are not suitable from an industrial point of view, due to the low deposition rates ( $\sim 1 \text{ \AA/s}$ ) and the actual difficulty in transferring the epitaxial layer away from the substrate (germanium), which is also reusable only few times. The latest technology under consideration, known as thin film (TF) photovoltaics, is very promising from an industrial perspective. Growth techniques employed for TF, such as High Vacuum Thermal Evaporation (HVTE), Close-Spaced Sublimation (CSS) and Radio Frequency Magnetron Sputtering (RFMS), enable high deposition rates ( $\sim 1 \mu\text{m/min}$ ) and cost reduction during production. There are two approaches for constructing the solar cell using TF technology: superstrate and substrate configurations (see fig. 1).

In superstrate configuration, solar photons must cross the substrate and the preceding layers before reaching the p-type absorber material. Typically, iron-free soda-lime glass,

which is transparent in the visible region of the solar spectrum, serves as substrate in this configuration [9]. In contrast, substrate configuration offers more adaptability, as the substrate can be opaque (*e.g.* ceramic) or even flexible [10].

Traditional materials used in thin-film technology include CdTe in the superstrate configuration and Cu(In,Ga)Se<sub>2</sub> (CIGS), in the substrate configuration, which have achieved competitive PCE of approximately 21% and 23.4%, respectively [1]. However, a significant drawback associated with CdTe and CIGS-based solar cells is the scarcity of tellurium, indium, and gallium in the Earth crust [11, 12] along with the toxicity of cadmium [13]. In this regard, it is important to note that while cadmium is toxic, the CdTe compound itself is extremely stable and non-toxic [14]. Research indicates that CdTe-based module exposed to rain releases cadmium in concentrations below the established safety thresholds. Furthermore, CdTe exhibits a melting point of about 1040 °C, a temperature that is rarely reached in typical fires.

To address the shortage of (expensive) basic elements, the PV community is looking for alternative p-type absorber materials and fabrication technologies. Among the approaches that have successfully contributed to the development of high-efficiency thin-film solar cells are:

- Organic solar cells, achieving the maximum PCE of 19.7% [15].
- Perovskite and perovskite quantum-dot based, with PCE record of 25.7% with small-area device [16] and 18.1%, respectively [17]
- Dye-Sensitized (DSSC) with a power conversion efficiency in the range 11–12% [18].

Another very promising approach is provided by antimony chalcogenides, with a particular focus on antimony selenide (Sb<sub>2</sub>Se<sub>3</sub>), which is the object of the work presented in this paper.

## 2. – Antimony selenide properties

Antimony selenide (ASe) is naturally a weakly p-type semiconductor [19] with a distinctive crystal structure. ASe crystallizes in an orthorhombic structure formed by covalent bonds between Se and Sb atoms along the *c*-axis ([001] direction), creating a ribbon-like structure. The neighbouring ribbons are held together by weak van der Waals Se-Se bonds [20, 21]. Sb<sub>2</sub>Se<sub>3</sub> is a very interesting material for photovoltaic applications due to its direct band gap of 1.2 eV [22], which aligns with the maximum of the Shockley-Queisser (S-Q) curve for the thermodynamic limit of efficiency (as shown in fig. 2).

Furthermore, Sb<sub>2</sub>Se<sub>3</sub> exhibits a high absorption coefficient in the visible region of the solar spectrum ( $\alpha \geq 10^5 \text{ cm}^{-1}$ ) [23], that allows growing ASe with relatively low thicknesses ( $\sim 800 \text{ nm}$ ) but very high absorbance.

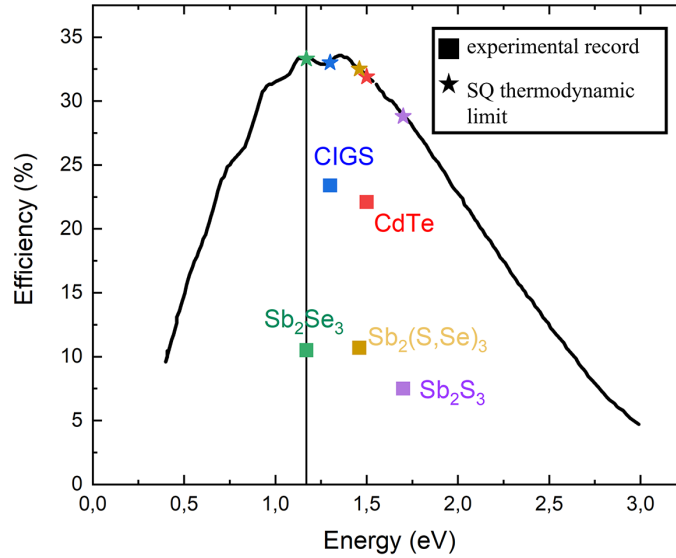


Fig. 2. – Shockley-Queisser limit for the different semiconductors typically employed in TF technology.

### 3. – The crystalline grain orientation

Antimony selenide examined in this work was grown by the CSS-technique, with the deposition parameters previously reported in [24, 25]. Solar cells in superstrate configuration were fabricated from such thin films, whose photovoltaic properties were seen to be closely linked to the growth of  $\text{Sb}_2\text{Se}_3$ , which, in turn, is highly dependent on the choice of the window layer material (the n-type material on which ASe is grown to form the p/n junction). The direction along which ASe grains grow significantly impacts the electron conduction. If the electron motion aligns with the direction of the ribbon-like structure, mobility values of approximately  $\mu \sim 9 \text{ cm}^2 \text{ V}^{-1} \text{ s}^{-1}$  can be reached [26].

Conversely, when the ASe grains grow along the [100] direction the mobility value is significantly lower, approximately in the range  $0.7\text{--}1.2 \text{ cm}^2 \text{ V}^{-1} \text{ s}^{-1}$  [27–29]. To control the ASe grain orientation, five different window layers (WL): CdS, CdS:F [30], CdSe,  $\text{As}_2\text{S}_3$  and  $\text{Zn}_{0.15}\text{Cd}_{0.85}\text{S}$  were produced and tested. These window layers play a crucial role in determining how ASe grains grow and, subsequently, affect the performance of the photovoltaic device.

As shown in fig. 3, the intensity of the selected XRD peaks of  $\text{Sb}_2\text{Se}_3$  exhibits significant variations when various window layers are used for growing ASe. Consequently, it is possible to establish a figure of merit, known as the texture coefficient (TC). The texture coefficient provides a quantification of how dominant a particular crystal plane is in comparison to others, as described in ref. [24].

$$\text{TC}_{hkl}\% = \frac{I_{hkl}/I_{h_0k_0l_0}}{\sum_{i=1}^n I_{h_i k_i l_i}/I_{h_0 i k_0 i l_0 i}} \times 100,$$

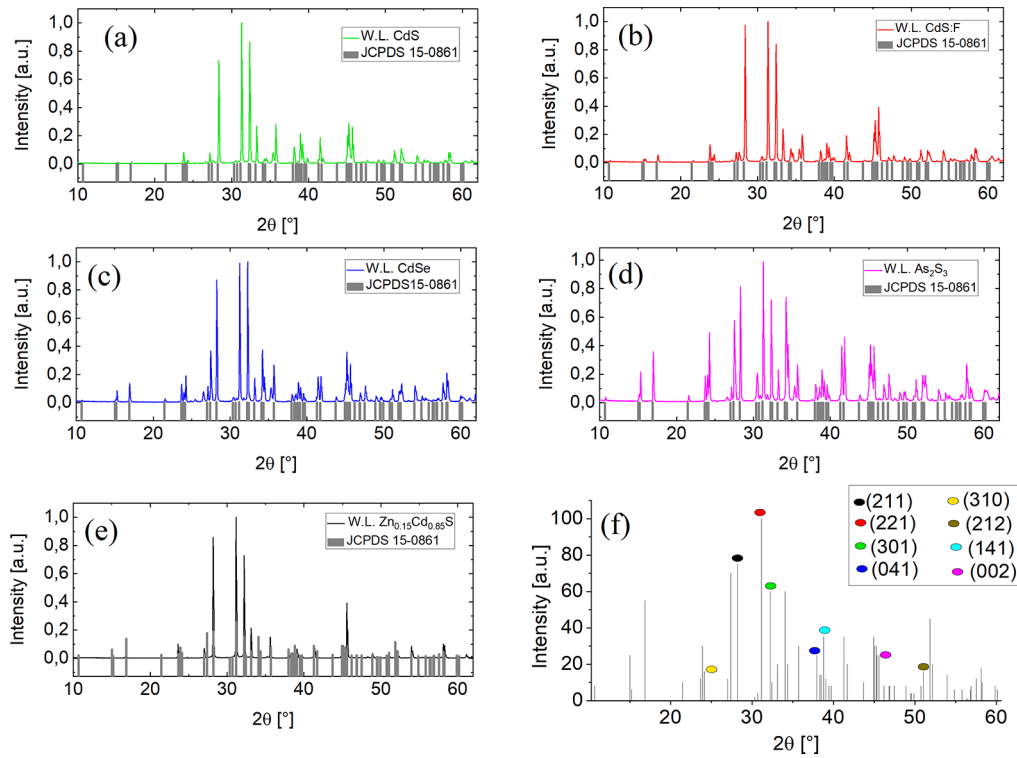


Fig. 3. – XRD patterns of antimony selenide (ASe) grown on various window layers: (a) CdS, (b) CdS:F, (c) CdSe, (d)  $\text{As}_2\text{S}_3$  and (e) ZnCdS. In the bottom right figure, the primary peaks of  $\text{Sb}_2\text{Se}_3$  have been indexed according to the PDF (Powder Diffraction File), providing a clear indication of the crystallographic structure of the material.

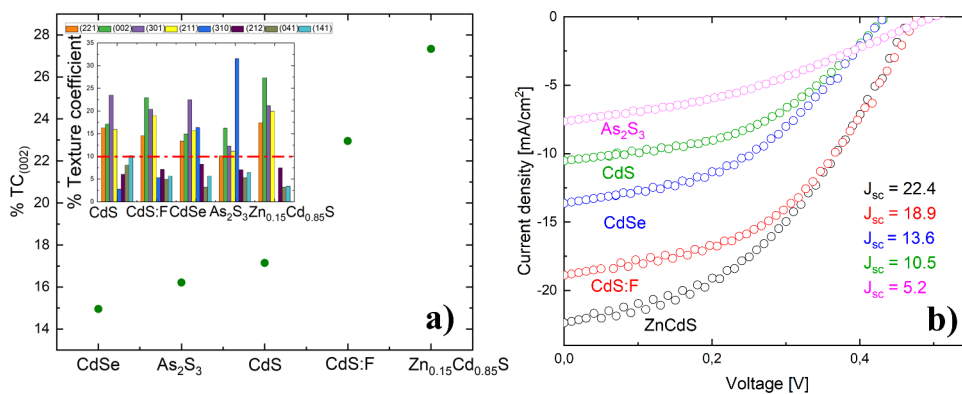


Fig. 4. – a) Preferential growth on the (002) plane is evident for all window layers. In the inset, the TC analysis is displayed, with a threshold value set at 10% to determine which crystallographic planes give the most significant contribution. b) Current-voltage characteristics of  $\text{Sb}_2\text{Se}_3$ -based solar cells grown on different window layers.

where  $I_{hkl}$ ,  $I_{h_0k_0l_0}$  and  $n$  are the experimental intensity of the selected peaks their theoretical intensity and the number of the peaks, respectively.

The (002) preferential growth plane becomes dominant when ZnCdS is used as the window layer, with a texture coefficient of  $TC_{(002)}\% \sim 27\%$ . In this scenario,  $Sb_2Se_3$  ribbons primarily grow along the [001] direction, which enhances carrier transport. This is supported by the correlation values of  $J_{sc}$  reported in fig. 4(b) for the different window layers.

#### 4. – Back-contact optimization

Optimizing the back-contact is a critical aspect to achieve high-performance solar cells. A good back-contact must meet two key requirements: it should exhibit Ohmic behaviour and have low resistivity. When dealing with a p-type semiconductor, the general guideline for selecting the metal material for making an Ohmic contact is the Schottky-Mott rule, which states that the work function of the metal must be higher than or equal to the electron affinity of the p-type semiconductor [31]. Meeting simultaneously all these requirements is challenging. Therefore, in thin-film solar cells, it is common practice to introduce a thin layer of semiconductor material with low energy gap and low resistivity (essentially, a p-type degenerate semiconductor) between the metal and the semiconductor. This intermediate layer helps to effectively align the energy band diagrams [32,33] thus ensuring the desired Ohmic behavior and low resistivity for efficient photocarrier collection in the solar cell.

In this study, an amorphous/nanostructured layer composed of a mixed phase of sulphur, oxygen, and iron (Fe-S-O) is introduced as the back-contact material. This layer is deposited by radio-frequency magnetron sputtering at room temperature (RT) [34]. The Seebeck effect analysis [35], performed on the Fe-S-O layer, grown on glass, demonstrated the p-type conductivity, while the resistivity at RT was determined to be  $1.3 \cdot 10^{-2} \Omega \text{ cm}$ , using the van der Pauw method [36]. To contact  $Sb_2Se_3$ , five contact strips of Au-coated Fe-S-O were deposited. This innovative back-contact approach aims at ensuring efficient charge transport and compatibility with the solar-cell structure.

The  $I$ - $V$  (current-voltage) characteristics measured for each pair of contacts, confirmed the Ohmic nature of the contact, as shown in fig. 5(a). A good contact must exhibit Ohmic behaviour but also provide low resistivity at the interface. However, due to the presence of grain boundaries and the vertical configuration of the device, it was not possible to determine the contact resistance through the traditional transmission line method measurement (TLM), as it may lead to overestimations.

The total series specific resistance (area independent, measured in  $\Omega \text{ cm}^2$ ) of the solar cell  $R_s$  can be expressed as the sum of the antimony selenide specific resistance ( $R_{sc}$ ) and the specific contact resistance ( $R_c$ )

$$R_s = R_{sc} + R_c.$$

Furthermore,  $R_{sc}$  can be written as the product of resistivity  $\rho_{sc}$  and thickness  $d$  of the

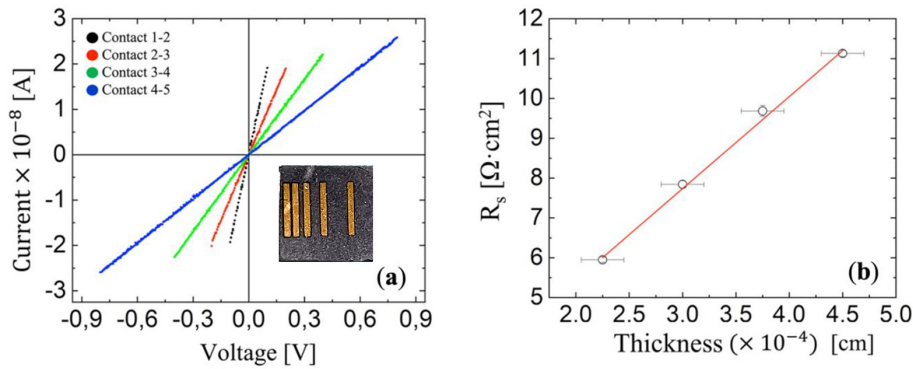


Fig. 5. – (a) Ohmic behaviour of FeSO+Au contact deposited on antimony selenide. In the inset a picture of TLM geometry is presented. (b) Linear fit of the total series resistance  $R_s$  vs. the thickness  $d$  of  $\text{Sb}_2\text{Se}_3$ . Data are obtained from solar cells with different  $\text{Sb}_2\text{Se}_3$  thickness, and they allow to estimate the specific contact resistance ( $R_c$ ). The information is derived from the source reference [34].

antimony selenide. Therefore, the previous equation can be expressed as

$$R_s = \rho_{sc} \cdot d + R_c.$$

By plotting  $R_s$  for a series of  $\text{Sb}_2\text{Se}_3$  samples with different thicknesses it is possible to extrapolate the specific contact resistance as intercept and the resistivity as slope of the plot. Examples of such plot are reported in fig. 5(b): a specific contact resistance of approximately,  $R_c \sim 0.8 \Omega \text{ cm}^2$  was determined. This value of contact resistivity is comparable with literature data for CdTe and CIGS-based solar cells [37, 38].

**4.1. Conclusion.** – This paper provides a survey of current limits in silicon solar-cell technology, and focuses on the potential advantages of thin-film solar cells. Attention was put on antimony selenide, a compound made of elements that are non-toxic and abundant on Earth. Furthermore, this paper includes a detailed discussion about grain orientation of the thin absorber and its significant influence on the performance of the solar cell.

These findings open new avenues for the development of more efficient and sustainable solar-cell technologies. A thorough investigation of the band alignment at the heterojunction interface is essential to further increase the cell performance. We showed that it is important to reduce the interface defects that may form at the interface between the window layer and the antimony selenide. Given the weak p-type conductivity of undoped  $\text{Sb}_2\text{Se}_3$  it is imperative, in future works, to explore methods for increasing the density of free carriers by introducing extrinsic dopants, such as iron or tin. This approach is crucial for the development of more efficient  $\text{Sb}_2\text{Se}_3$ -based solar cells.

## REFERENCES

- [1] GREEN M. A., DUNLOP E. D., SIEFER G., YOSHITA M., KOPIDAKIS N., BOTHE K. and HAO X., “Solar cell efficiency tables (Version 61)”, *Progr. Photovoltaics: Res. Appl.*, **31** (2023) 3, <https://doi.org/10.1002/pip.3646>.
- [2] BATHEY B. R. and CRETELLA M. C., “Solar-grade silicon”, *J. Mater. Sci.*, **17** (1982) 3077, <https://doi.org/10.1007/BF01203469>.
- [3] RANJAN S., BALAJI S., PANELLA R. A. and YDSTIE B. E., “Silicon solar cell production”, *Comput. Chem. Eng.*, **35** (2011) 1439, <https://doi.org/10.1016/j.compchemeng.2011.04.017>.
- [4] RAJKANAN K., SINGH R. and SHEWCHUN J., “Absorption coefficient of silicon for solar cell calculations”, *Solid State Electron.*, **22** (1979) 793, [https://doi.org/10.1016/0038-1101\(79\)90128-X](https://doi.org/10.1016/0038-1101(79)90128-X).
- [5] SOPORI B. L. and PRYOR R. A., “Design of antireflection coatings for textured silicon solar cells”, *Solar Cells*, **8** (1983) 249, [https://doi.org/10.1016/0379-6787\(83\)90064-9](https://doi.org/10.1016/0379-6787(83)90064-9).
- [6] YEROKHOV V. Y., HEZEL R., LIPINSKI M., CIACH R., NAGEL H., MYLYANYCH A. and PANEK P., “Cost-effective methods of texturing for silicon solar cells”, *Solar Energy Mater. Solar Cells*, **72** (2002) 291, [https://doi.org/10.1016/S0927-0248\(01\)00177-5](https://doi.org/10.1016/S0927-0248(01)00177-5).
- [7] NIJS J. F., SZLUFCHIK J., POORTMANS J. and SIVOTHTHAMAN S., “Advanced manufacturing concepts for crystalline silicon solar cells”, *IEEE Trans. Electron Devices*, **46** (1999) 1948, <https://doi.org/10.1109/16.791983>.
- [8] GEISZ J. F., FRANCE R. M., SCHULTE K. L., STEINER M. A., NORMAN A. G., GUTHREY H. L., YOUNG M. R., SONG T. and MORIARTY T., “Six-junction III–V solar cells with 47.1% conversion efficiency under 143 Suns concentration”, *Nat. Energy*, **5** (2020) 326, <https://doi.org/10.1038/s41560-020-0598-5>.
- [9] GASPARI F. and QUARANTA S., “Photovoltaic Materials”, *Comprehens. Energy Syst.*, **2–5** (2018) 117, <https://doi.org/10.1016/B978-0-12-809597-3.00215-7>.
- [10] ROMEO A., “CdTe Solar Cells”, *McEvoy’s Handbook of Photovoltaics: Fundamentals and Applications* (Elsevier) 2018, pp. 309–369, <https://doi.org/10.1016/B978-0-12-809921-6.00009-4>.
- [11] ZHANG X., XU W., WANG S., LIU D., DENG P., DENG J. and JIANG W., “Research Status of Recovery of Tellurium from Cadmium Telluride Photovoltaic Modules”, *IOP Conf. Ser. Mater. Sci. Eng.*, **782** (2020) 022024, <https://doi.org/10.1088/1757-899X/782/2/022024>.
- [12] SELMANE N., CHEKNANE A., KHEMLOUL F., HELAL M. H. S. and HILAL H. S., “Cost-saving and performance-enhancement of CuInGaSe solar cells by adding CuZnSnSe as a second absorber”, *Solar Energy*, **234** (2022) 64, <https://doi.org/10.1016/j.solener.2022.01.072>.
- [13] FTHENAKIS V. M. and BULAWKA A. O., “Photovoltaics, Environmental Impact of”, *Encyclopedia of Energy*, Vol. **5**, (Elsevier) 2004, pp. 61–69, <https://doi.org/10.1016/B0-12-176480-X/00421-6>.
- [14] ROMEO A. and ARTEGIANI E., “CdTe-Based Thin Film Solar Cells: Past, Present and Future”, *Energies (Basel)*, **14** (2021) 1684, <https://doi.org/10.3390/en14061684>.
- [15] LIU K., JIANG Y., RAN G., LIU F., ZHANG W. and ZHU X., “19.7% efficiency binary organic solar cells achieved by selective core fluorination of nonfullerene electron acceptors”, *Joule*, **8** (2024) 835, <https://doi.org/10.1016/j.joule.2024.01.005>.
- [16] FU Q. and JEN A. K. Y., “Perovskite solar cell developments, what’s next?”, *Next Energy*, **1** (2023) 100004, <https://doi.org/10.1016/j.nxener.2023.100004>.

- [17] HAO M., DING S., GAZNAGHI S., CHENG H. and WANG L., “Perovskite Quantum Dot Solar Cells: Current Status and Future Outlook”, *ACS Energy Lett.*, **9** (2024) 308, <https://doi.org/10.1021/acsenergylett.3c01983>.
- [18] SEKARAN P. D. and MARIMUTHU R., “An Extensive Analysis of Dye-Sensitized Solar Cell (DSSC)”, *Braz. J. Phys.*, **54** (2023) 28, <https://doi.org/10.1007/s13538-023-01375-w>.
- [19] LIU X., XIAO X., YANG Y., XUE D. J., LI D. B., CHEN C., LU S., GAO L., HE Y., BEARD M. C., WANG G., CHEN S. and TANG J., “Enhanced  $\text{Sb}_2\text{Se}_3$  solar cell performance through theory-guided defect control”, *Progr. Photovolt.: Res. Appl.*, **25** (2017) 861, <https://doi.org/10.1002/pip.2900>.
- [20] MAVLONOV A., RAZYKOV T., RAZIQ F., GAN J., CHANTANA J., KAWANO Y., NISHIMURA T., WEI H., ZAKUTAYEV A., MINEMOTO T., ZU X., LI S. and QIAO L., “A review of  $\text{Sb}_2\text{Se}_3$  photovoltaic absorber materials and thin-film solar cells”, *Solar Energy*, **201** (2020) 227, <https://doi.org/10.1016/j.solener.2020.03.009>.
- [21] TIDESWELL N. W., KRUSE F. H. and MCCULLOUGH J. D., “The crystal structure of antimony selenide,  $\text{Sb}_2\text{Se}_3$ ”, *Acta Crystallogr.*, **10** (1957) 99, <https://doi.org/10.1107/S0365110X57000298>.
- [22] GHOSH S., MOREIRA M. V. B., FANTINI C. and GONZÁLEZ J. C., “Growth and optical properties of nanocrystalline  $\text{Sb}_2\text{Se}_3$  thin-films for the application in solar-cells”, *Solar Energy*, **211** (2020) 613, <https://doi.org/10.1016/J.SOLENER.2020.10.001>.
- [23] CHEN C., LI W., ZHOU Y., CHEN C., LUO M., LIU X., ZENG K., YANG B., ZHANG C., HAN J. and TANG J., “Optical properties of amorphous and polycrystalline  $\text{Sb}_2\text{Se}_3$  thin films prepared by thermal evaporation”, *Appl. Phys. Lett.*, **107** (2015) 043905, <https://doi.org/10.1063/1.4927741>.
- [24] PASINI S., SPOLTRE D., PARISINI A., FOTI G., MARCHIONNA S., VANTAGGIO S., FORNARI R. and A. BOSIO, “ $\text{Sb}_2\text{Se}_3$  Polycrystalline Thin Films Grown on Different Window Layers”, *Coatings*, **13** (2023) 338, <https://doi.org/10.3390/coatings13020338>.
- [25] ROMEO N., BOSIO A., CANEVARI V. and PODESTÀ A., “Recent progress on CdTe/CdS thin film solar cells”, *Solar Energy*, **77** (2004) 795, <https://doi.org/10.1016/j.solener.2004.07.011>.
- [26] LI Y., ZHOU Y., ZHU Y., CHEN C., LUO J., MA J., YANG B., WANG X., XIA Z. and TANG J., “Characterization of Mg and Fe doped  $\text{Sb}_2\text{Se}_3$  thin films for photovoltaic application”, *Appl. Phys. Lett.*, **109** (2016) 232104, <https://doi.org/10.1063/1.4971388>.
- [27] CHEN C., BOBELA D. C., YANG Y., LU S., ZENG K., GE C., YANG B., GAO L., ZHAO Y., BEARD M. C. and TANG J., “Characterization of basic physical properties of  $\text{Sb}_2\text{Se}_3$  and its relevance for photovoltaics”, *Front. Optoelectron.*, **10** (2017) 18, <https://doi.org/10.1007/s12200-017-0702-z>.
- [28] CHEN C., LI K. and TANG J., “Ten Years of  $\text{Sb}_2\text{Se}_3$  Thin Film Solar Cells”, *Solar RRL*, **6** (2022) 2200094, <https://doi.org/10.1002/solr.202200094>.
- [29] ZHOU Y., WANG L., CHEN S., QIN S., LIU X., CHEN J., XUE D.-J., LUO M., CAO Y., CHENG Y., SARGENT E. H. and TANG J., “Thin-film  $\text{Sb}_2\text{Se}_3$  photovoltaics with oriented one-dimensional ribbons and benign grain boundaries”, *Nat. Photon.*, **9** (2015) 409, <https://doi.org/10.1038/nphoton.2015.78>.
- [30] ROMEO N., BOSIO A. and CANEVARI V., “The role of CdS preparation method in the performance of CdTe/CdS thin film solar cell”, *Proceedings of the 3rd World Conference on Photovoltaic Energy Conversion, Osaka, Japan, 2003*, Vol. 1, pp. 469-470.
- [31] TUNG R. T., “The physics and chemistry of the Schottky barrier height”, *Appl. Phys. Rev.*, **1** (2014) 011304, <https://doi.org/10.1063/1.4858400>.
- [32] ROMEO N., BOSIO A., CANEVARI V. and PODESTÀ A., “Recent progress on CdTe/CdS thin film solar cells”, *Solar Energy*, **77** (2004) 795, <https://doi.org/10.1016/j.solener.2004.07.011>.

- [33] ZHANG M.-J., LIN Q., YANG X., MEI Z., LIANG J., LIN Y. and PAN F., “Novel p-Type Conductive Semiconductor Nanocrystalline Film as the Back Electrode for High-Performance Thin Film Solar Cells”, *Nano Lett.*, **16** (2016) 1218, <https://doi.org/10.1021/acs.nanolett.5b04510>.
- [34] PASINI S., SPOLTORE D., PARISINI A., MARCHIONNA S., FORNASINI L., BERSANI D., FORNARI R. and BOSIO A., “Innovative back-contact for Sb<sub>2</sub>Se<sub>3</sub>-based thin film solar cells”, *Solar Energy*, **249** (2023) 414, <https://doi.org/10.1016/j.solener.2022.11.049>.
- [35] PANG C. S. B., NG W., LIANG J., QU Q., CHAU H. T. M., NIU M., CHENG M. K. and SOU I. K., “A Simple Thermoelectric Effect Setup for Determining the Conductivity Type of Thin Film Materials”, *IEEE Trans. Instrum. Meas.*, **70** (2021) 1502007, <https://doi.org/10.1109/TIM.2020.3046922>.
- [36] VAN DER PAUW L. J., “A method of measuring specific resistivity and Hall effect of discs of arbitrary shape”, in: *Semiconductor Devices: Pioneering Papers*, edited by S. M. Sze (World Scientific), pp. 174–182. [https://doi.org/10.1142/9789814503464\\_0017](https://doi.org/10.1142/9789814503464_0017).
- [37] CORDES H. and SCHMID-FETZERT R., “Electrical properties and contact metallurgy of elemental (Cu, Ag, Au, Ni) and compound contacts on p-Cd<sub>0.95</sub>Zn<sub>0.05</sub>Te”, *Semicond. Sci. Technol.*, **10** (1995) 77, <https://doi.org/10.1088/0268-1242/10/1/013>.
- [38] ASSMANN L., BERNÈDE J. C., DRICI A., AMORY C., HALGAND E. and MORSLI M., “Study of the Mo thin films and Mo/CIGS interface properties”, *Appl. Surf. Sci.*, **246** (2005) 159, <https://doi.org/10.1016/j.apsusc.2004.11.020>.